Iron corrosion induced by the hyperthermophilic sulfate-reducing archaeon Archaeoglobus fulgidus at 70°C

Oulfat Amin Ali, Emmanuel Aragon, Armand Fahs, Sylvain Davidson, Bernard Ollivier, Agnès Hirschler-Réa

Iron corrosion induced by the hyperthermophilic sulfate-reducing archaeon *Archaeoglobus fulgidus* at 70 °C

Oulfat Amin Ali [a,*], Emmanuel Aragon [b], Armand Fahs [b], Sylvain Davidson [a], Bernard Ollivier [a], Agnès Hirschler-Rea [a]

[a] *Aix Marseille Univ., Université de Toulon, CNRS, IRD, MIO UM 110, 13288, Marseille, France*
[b] *MAPIEM Laboratory (EA 4323), University of Toulon, CS 60584, 83041, Toulon Cedex 9, France*

ARTICLE INFO

Keywords:
Iron biocorrosion
Chimneys
Hyperthermophile
A. fulgidus
Sulfate-reducing archaeon
Biofilm

ABSTRACT

This work assessed the role of the hyperthermophilic sulfate-reducing archaeon, *Archaeoglobus fulgidus* in anaerobic iron corrosion, at 70 °C, in the presence and the absence of lactate as energy source. Experiments performed with *A. fulgidus* planktonic cells, displayed their capacity to form a biofilm on an iron coupon and exhibited their biocorrosive activity. *A. fulgidus* was shown to cause indirect corrosion by producing sulfide while oxidizing lactate. Furthermore, the archaeon could grow lithotrophically by using elemental iron as a mineral energy source. Under these latter conditions, *A. fulgidus* formed chimneys enhancing the direct corrosion process. Moreover, physiological modifications occurred under these conditions notably highlighting the probable use of CO_2 instead of sulfate as a terminal electron acceptor to produce acetate similarly to homoacetogens. All together, these results illustrate the metabolic versatility and hence the importance of this hyperthermophilic archaeon in microbial induced corrosion (MIC).

1. Introduction

Corrosion is commonly defined as natural oxidation with subsequent deterioration of metals and alloys (Perez, 2004; Videla and Herrera, 2005). As a metal, iron is very unstable in aqueous media. Therefore, it dissolves in water according to the following reaction:

$$4\ Fe^0 \leftrightarrow 4\ Fe^{2+} + 8\ e^-;\ E^0 = -447\ mV \quad (1)$$

The metallic surface works as an electrochemical cell combining an anodic site and a cathodic site where oxidation and reduction reactions occur, respectively, allowing an electron flow from anode to cathode (Enning and Garrelfs, 2014; Sherar et al., 2013). In oxic environments, electrons that result from Fe^0 oxidation reduce molecular oxygen and lead to rust or the formation of iron oxides. This aerobic corrosive process is mainly attributed to electrochemical reactions (Enning and Garrelfs, 2014; Sherar et al., 2013; Liengen et al., 2014). In anoxic conditions, electrons that result from Fe^0 oxidation reduce protons from dissociated water. However, this chemical iron oxidation coupled to proton reduction usually remains low (Enning and Garrelfs, 2014; Enning et al., 2012; Kaesche, 2012) in environments lacking oxygen or acid and metallic facilities (Enning and Garrelfs, 2014). Nevertheless, microorganisms drastically accelerate this phenomenon, and anaerobic corrosion mainly results from either microbial activity or the end products of their metabolism (Videla and Herrera, 2005; Cord-Ruwisch and Widdel, 1986; Dinh et al., 2004; Zhang et al., 2015; Liang et al., 2016). More than 20% of all corrosion loss is recognized to be of microbial origin and is referred to as microbiologically influenced corrosion (MIC) (Zhang et al., 2015; Hamilton, 2003; Dang and Lovell, 2016; Beech and Sunner, 2004). Commonly, microorganisms adhere to metallic surfaces by forming a biofilm, which enables MIC through two mechanisms: (i) indirect corrosion by producing corrosive compounds such as sulfides, which provoke chemical attacks on iron, and (ii) direct corrosion by oxidizing Fe^0 and pulling electrons to reduce electron acceptors (Enning et al., 2012; Van Ommen Kloeke et al., 1995; Mehanna et al., 2009; Venzlaff et al., 2013). In direct corrosion, several theories were proposed among which the so called “cathodic depolarization” (Von Wolzogen Kuehr C and van der Vlugt L, 1964). This theory suggests that H_2 resulting from the reduction of dissolved protons in water would builds-up a “hydrogen film” (Venzlaff et al., 2013). In presence of hydrogenotrophic microorganisms, such as sulfate-reducing bacteria (SRB), it has been speculated that hydrogen formed on metallic surface

* Corresponding author.
E-mail addresses: oulfat.aminali@gmail.com (O. Amin Ali), emmanuel.aragon@univ-tln.fr (E. Aragon), armand.fahs@univ-tln.fr (A. Fahs), sylvain.davidson@mio.osupytheas.fr (S. Davidson), bernard.ollivier@mio.osupytheas.fr (B. Ollivier), agnes.hirschler-rea@mio.osupytheas.fr (A. Hirschler-Rea).

Abbreviations

$\mu A/cm^2$	microampere per square centimeter
µm	µ-meter
AFM	Atomic force microscopy
ANOVA	Analysis of variance
BES	Basic electrochemical system
Cm^2	Square centimeter
Ecorr	Corrosion potential
EDX	Energy dispersive X-rays
$g{\cdot}L^{-1}$	Grams per liter
HPLC	High-performance liquid chromatography
Hz	Hertz
kHz	Kilohertz
Kv	Kilovolt
L:	Liter
M	Mole
MIC	Microbiologically influenced corrosion
$ml{\cdot}L^{-1}$	milliliter per Liter
mV	Milivolt
nd	non-detected
nm	nanometer
SAE	Society of Automotive Engineers
SCE	Saturated calomel electrode
SEM	Scanning electron microscopy
Si	Silicon
SPM	Scanning probe microscope
UV	Ultraviolet
Vol	Volume
ΔE	Delta of potential

can be scavenged by SRB thus facilitating the oxidative process (Von Wolzogen Kuehr C and van der Vlugt L, 1964). However, this theory has been extensively questioned as it cannot affect or accelerate iron corrosion based on kinetics and thermodynamics perspectives (Enning and Garrelfs, 2014; Liang et al., 2016; Costello, 1974; Vigneron et al., 2016).

Many microbial groups such as acetogenic bacteria (Enning and Garrelfs, 2014; Kato et al., 2015; Mand et al., 2014, 2015), nitrate-reducing bacteria (Enning and Garrelfs, 2014; Hubert et al., 2005), sulfate and thiosulfate-reducing prokaryotes (Enning and Garrelfs, 2014; Liang et al., 2016; Magot et al., 1997) and methanogenic archaea (Costello, 1974; Vigneron et al., 2016; Mand et al., 2015; Davidova et al., 2012; Liang et al., 2014) have been identified as being involved in MIC. While MIC has been widely studied in sulfate-reducing bacteria (e.g., *Desulfovibrio* spp.) that are known to be widespread in natural environments (Enning and Garrelfs, 2014; Zhang et al., 2015; Hamilton, 2003; Dang and Lovell, 2016; Beech and Sunner, 2004; Van Ommen Kloeke et al., 1995), very few studies regarding sulfate-reducers belonging to the *Archaea* domain have been reported. Within the *Archaea,* sulfur-reducing, non-sulfate-reducing and sulfide-producing hyperthermophilic members of the order *Thermococcales* (e.g., *Thermococcus* spp.), which grow in co-culture with hydrogenotrophic methanogens, were demonstrated to be highly corrosive (Davidova et al., 2012; Liang et al., 2014; Duncan et al., 2009). They were also found to be biocorrosive in enrichment cultures in the presence of thiosulfate as a terminal electron acceptor (Liang et al., 2014). In this respect, anaerobic hyperthermophilic *Archaea* representatives, and in particular sulfate-reducing archaea such as *Archaeoglobus* species, may be active contributors to corrosion at high temperature, notably in oilfield facilities and hot oil reservoirs where their presence has been demonstrated on several occasions (Enning and Garrelfs, 2014; Davidova et al., 2012; Duncan et al., 2009; Ollivier and Magot, 2005).

Archaeoglobus fulgidus is a hyperthermophilic sulfate-reducing archaeon that has been isolated from shallow submarine hot vents in the Mediterranean Sea (Stetter, 1988), volcanic environments (Zellner et al., 1989), various hot oil field waters in the North Sea (Stetter et al., 1993; Beeder et al., 1994), a continental reservoir (L'Haridon et al., 1995) and a deep aquifer basin (Fardeau et al., 2009). One of the most studied and well-characterized strain is *A. fulgidus* VC-16, which was the first sulfur-metabolizing archaeon whose genome was sequenced (Klenk et al., 1997; Henstra et al., 2007; Hocking et al., 2014). It is an organotrophic and lithoautotrophic archaeon that grows on a variety of energy sources including lactate, hydrogen, and carbon monoxide (Stetter, 1988; Klenk et al., 1997; Vornolt et al., 1995) as well as aliphatic hydrocarbons (Khelifi et al., 2010, 2014). In addition to sulfate, thiosulfate and sulfite are also used as terminal electron acceptors (Stetter, 1988). Notably, hydrogen is only oxidized in the presence of thiosulfate (Stetter, 1988; Klenk et al., 1997). Interestingly, the ability of *A. fulgidus* to form biofilms under stress conditions such as metal-enriched environment was demonstrated (Lapaglia and Hartzell, 1997). Therefore, *A. fulgidus* VC-16 represents a good candidate to study anaerobic biocorrosion processes at high temperature. Indeed, Islam & Karr had reported the corrosive ability of *A. fulgidus* by measuring weight loss (Islam and Karr, 2013). Besides, Jia et al. (2018), recently, performed a corrosion study with *A. fulgidus*. In their experiments, a robust biofilm initially developed on an iron coupon with organic matter in an enriched seawater medium. This mature biofilm was then exposed to different conditions of carbon starvation. They showed that the formed biofilm was very corrosive under organic carbon starvation and that the sulfate-reducing archaeon was able to use elemental iron as an electron donor (Jia et al., 2018).

In this work, planktonic cells of *A. fulgidus* were grown in a mineral culture medium containing a carbon steel coupon in presence and absence of an organic electron donor and with sulfate as terminal electron acceptor. The aim of the study is to deepen our understanding of the mechanisms of direct and/or indirect corrosion by *A. fulgidus* VC-16 and, specifically, under oligotrophic conditions, which are encountered, more particularly, in oilfield waters.

2. Materials and methods

2.1. Metal sample preparation

Coupons (Control 5, Mexico) made of SAE 1010 carbon steel (127 mm × 12.7 mm x 0.25 mm) served as the source of metallic iron. Beside Fe, their mass percentage composition is (wt %) C 0.10, Mn 0.45, P 0.04, S 0.05. These metallic coupons were mirror-polished by a specialized subcontractor (CHROMALU) and surface-activated for 2 min in diluted HCl (2 M) until the formation of a substantial amount of hydrogen bubbles. Each steel coupon was then rinsed immediately three times in distilled water for 10 s, sterilized by UV light for 20 min on each side and stocked in a drying chamber.

2.2. Growth of A. fulgidus VC-16

Archaeoglobus. fulgidus strain VC-16 (DSM 4304) was isolated from a marine hydrothermal vent (Stetter, 1988). It was provided by the Deutsche Sammlung von Mikroorganismen und Zellkulturen (Braunschweig, Germany). It was cultured in a defined culture medium (Khelifi et al., 2010) that was modified as follows ($g{\cdot}L^{-1}$ unless indicated): NH_4Cl, 0.3; KCl, 0.1; $CaCl_2{\cdot}2H_2O$, 0.1; NaCl, 18; Na_2SO_4, 2.37; yeast extract, 0.1; $Fe_2SO_4{\cdot}7H_2O$, 1.42 mg; $NiSO_4{\cdot}6H_2O$, 1.6 mg; $Na_2WO_4{\cdot}2H_2O$, 38 µg; $Na_2SeO_3{\cdot}5H_2O$, 3 µg; MOPS, 3 g; resazurin, 1 mg and Balch trace element solution (Balch et al., 1979), 10 ml L^{-1}. The pH

of the medium was adjusted to 7.0. The medium was prepared anoxically in penicillin bottles with a headspace of N_2–CO_2 (4:1). Following sterilization, the medium was amended with sodium carbonate (2 g. L^{-1}), sodium thioglycolate (0.2 g L^{-1}), sodium ascorbate (0.2 g L^{-1}), $MgCl_2{\cdot}6H_2O$ (3.0 g L^{-1}), 10 ml L^{-1} of a vitamin solution (Wolin et al., 1963) and lactate (10 mM), except when stated.

The present medium was optimized to enable only biological response to corrosion process. Indeed, Na_2S, and L-cysteine commonly used as oxygen scavengers were removed from the medium because they cause rapid chemical corrosion. They were replaced by sodium thioglycolate and sodium ascorbate, which are completely harmless on carbon steel. Moreover, since KH_2PO_4 and K_2HPO_4 distorted electrochemical signals, they were replaced by MOPS to buffer the culture medium. Actually, the medium was optimized to enable only biological response to corrosion process.

Precultures were inoculated at 10% (vol/vol) under anoxic conditions and incubated for 2 days at 70 °C.

2.3. Corrosion tests

Corrosion tests were performed in 25-ml Bellco tubes filled with *A. fulgidus* culture medium. A metallic coupon and/or lactate were added to the sterilized culture medium. *A. fulgidus* inoculum was washed once with substrate-free medium before being added at 10% v/v. The tubes were filled completely and incubated horizontally at 70 °C so the biofilm of *A. fulgidus* could develop on the larger surface of the metallic coupon in biological assays. The same inoculum was added to all assays. Corrosion test kinetics and analyses were carried out in one shot experiment where 4 conditions, in presence and absence of iron coupon, were performed: (i) abiotic, (ii) abiotic with lactate, (iii) *A. fulgidus*, (iv) *A. fulgidus* with lactate. Three tubes were sacrificed per condition for each time of monitoring.

2.4. Chemical measures and analyses

The sulfate concentration was quantified by ion chromatography (761 Compact IC Metrohm, Metrohm) using a Metrosep Anion Supp1 column (Metrohm). The lactate (electron donor) and acetate (end-product of lactate oxidation) concentrations were determined by HPLC (Thermo Scientific) using an Aminex HPX-87H-300 x 7.8 column (Bio-Rad). The concentration of soluble Fe^{2+} was measured using the colorimetric method described by Lovley et al. (Lovley and Phillips, 1986) after solubilization of the black precipitate for approximately 5 min with 0.35 M HCl.

2.5. Scanning electron microscopy and elemental identification

Iron coupons were incubated for 20 days in *A. fulgidus*-inoculated culture medium. A 1 cm^2 coupon surface was cut from each crust-covered specimen and fully dried before scanning electron microscopy (SEM). SEM was performed in secondary electron imaging mode (SE2) with acceleration voltage of 5 kV, using a Zeiss Supra 40 VP microscope, equipped with a GEMINI column and coupled with an X-max 20 mm^2 energy-dispersive X-ray analyzer (Oxford Instruments). To observe pits, the corrosion crusts were removed by immersion in a 6 M hexamethylenetetramine-HCl solution with 3 M NH_4Cl for 5 min. After immersion, the iron specimens were rubbed with a toothbrush, rinsed with water and fully dried.

2.6. Atomic force microscopy

Topographic images of surface were recorded with an Atomic Force Microscopy (AFM) in intermittent contact mode. AFM experiments were performed in air using a Multimode AFM with Nanoscope V SPM controller. Silicon cantilever was used with a spring constant of 40 N m^{-1} and a resonant frequency of around 300 kHz. All images were collected with a resolution of 512 × 512 pixels and a scan rate of 0.5 Hz. Specimens were cleaned as explained above, dried and then characterized by AFM.

2.7. Electrochemical measurements and characterization

Experiments were carried out in a 1 L K0047 corrosion cell kit (AMETEK) that was sterilized with 96% ethanol prior to use. 0.8 L of sterile medium was added and purged by a stream of sterile N_2–CO_2 (80:20) gas for 2–3 h prior to inoculation and first measurement. The corrosion cell was subsequently tightly closed and placed into a polyethylene glycol bath at 70 °C for approximately 40 min. The latter step allowed the culture medium to reach and maintain the growth temperature of *A. fulgidus*. A 1 cm^2 working electrode (iron coupon) was exposed to the culture medium (electrolyte), the reference electrode was a saturated calomel electrode (SCE) and a graphite rod served as a counter electrode. Electrochemical experiments were carried out using a potentiostat/galvanostat (BES EG®&R), and data were acquired using Softcorr III software. The free corrosion potential E_{corr} was followed by connecting the working and reference electrodes of the electrochemical cell during their incubation in the electrolyte. After 8 days, E_{corr} monitoring was stopped and followed by linear sweep voltammetry. The latter was performed over a range of $\Delta E = -600$ mV–800 mV at a rate of 0.166 mV s^{-1}, starting 50 mV beneath the E_{corr}. Electrochemical characterization was performed to compare the four conditions cited above (*Cf. 2.3*).

2.8. Statistical analyses

The significance of the results was examined by multifactor analysis of variance for concentration (ANOVA) followed by post hoc tests (Fisher's least significant difference tests). These analyses were performed using STATGRAPHICS Centurion XVI.II. $P < 0.05$ was considered statistically significant.

3. Results

To explore the initiation timeline of corrosion, *A. fulgidus* VC-16 was grown with lactate and/or an iron coupon as electron donor(s) and sulfate as a terminal electron acceptor at 70 °C for three weeks. These assays were compared to abiotic controls that contained an iron coupon and sulfate either in presence or in absence of lactate. Both assays and controls were incubated under the same experimental conditions. Experimental settings used in the whole study were optimized to avoid any biasness of the biological response to corrosion. For instance, oxygen scavenger or modulators of electrochemical measurements have been removed and replaced by neutral components (see material and methods).

3.1. Iron surface crust

After three weeks of incubation at 70 °C, iron surfaces were observed by SEM to assess development of *A. fulgidus* on the metallic coupon. Observations showed that precipitates had accumulated on the steel surface of abiotic controls (Fig. 1B) and *A. fulgidus*-inoculated assays (Fig. 1C and D). When compared to non-incubated metal reference (Fig. 1A), the iron coupon surface incubated in the culture medium was covered by a thick black crust (Fig. 1B). No difference was observed between the abiotic controls containing an iron coupon, sulfate, with or without lactate. Thus, only the abiotic control with lactate was represented. Aside from the crust produced on the abiotic control (Fig. 1B), tangled materials were observed on the coupons from the *A. fulgidus*-inoculated assays in the presence of lactate (Fig. 1C). These tangled materials were less developed when lactate was lacking in the culture medium (Fig. 1D). Besides, particular chimney-like structures were observed, in the latter (Fig. 1D). Within 3 weeks, *A. fulgidus* grown on

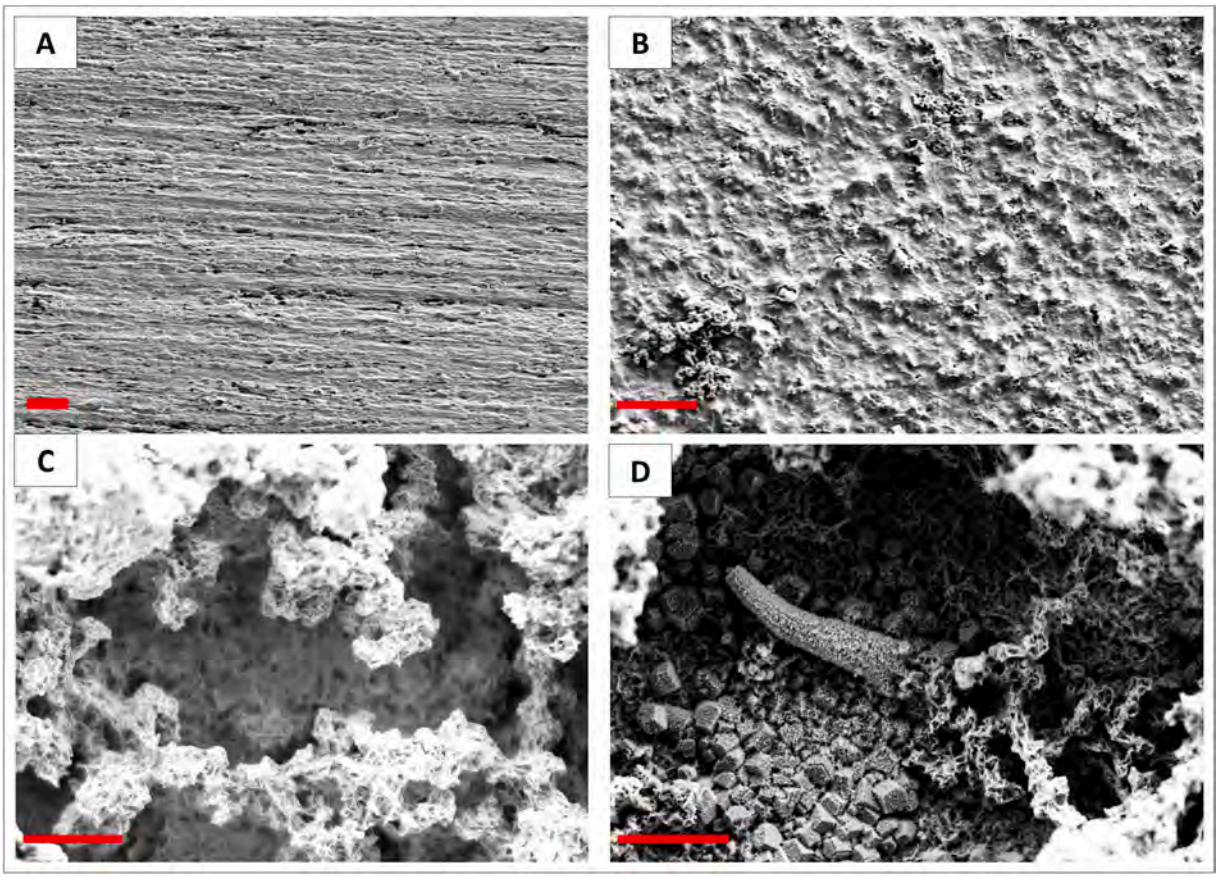

Fig. 1. Scanning electron micrographs (SEM) of crusts on iron surfaces after incubation for 3 weeks. (A) non-incubated metal reference; (B) abiotic control; (C) *A. fulgidus* with lactate; and (D) *A. fulgidus* without lactate showing a chimney (bars, 10 μm).

iron coupon developed a microbial biofilm supported by the presence of tangled materials (Fig. 1C–D).

3.2. Iron surface deposits composition

Composition of materials and crusts deposited on iron surfaces (Fig. 1B–D) was analyzed by energy-dispersive X-ray spectroscopy (EDX). The tangled material in *A. fulgidus* containing lactate assays (Fig. 1C) revealed that high mass percent of Fe (42.4%), S (14.8%), O (14.1%) and C (12.5%) constituted these filamentous materials. Other elements such as Na (8%), Cl (4.5%), Si (2.7%) and Mg (1.3%) were also identified at lower concentrations (Table 1). The composition of crust in abiotic control (Fig. 1B) was quite different with very low concentrations of S (1.9%) and Si (0.4%) elements. In comparison, chimneys observed in lactate lacking assays (Fig. 1D) contained no Si and low S elements (1%). However, in these assays without lactate, Si and S were present but mainly in the filamentous tangled materials underneath the chimneys as revealed by SEM-EDX analyses (Fig. 2). Furthermore, theses analyses confirmed that the *A. fulgidus* chimneys were mainly composed of Fe, C, O, Na, and Mg (Fig. 2 and Table 1). Our data provide clear evidence that composition of deposits differs between the conditions studied.

3.3. Corrosion pits

The selective removal of the crust from iron coupons was performed to observe corrosion damages. SEM observations revealed clear changes of the metal surface aspect for treated iron coupons with different types of pits (Fig. 3). In addition, AFM images illustrated that these metallic coupons had rugged topographies, confirming the SEM observations (Fig. 3A–D). In the abiotic control (Fig. 3B), AFM analysis showed pits with depths of up to 700 nm and 1–2 μm widths. Although pits on the metal incubated with *A. fulgidus* had same depths to that of the abiotic control, they were two-fold wider (Fig. 3C). These pits were deeper and wider when organic electron donor was added to the culture medium (Fig. 3D).

3.4. Electrochemical activity of A. fulgidus on iron coupon

3.4.1. Effect of A. fulgidus on the free corrosion potential of iron

Electrochemical potential/time characterizations were carried out to assess deterioration of the metallic surface when it was immersed in *A. fulgidus* culture medium. Indeed, open circuit potential (E_{corr}) was monitored for 1 cm^2 immersed iron coupon in inoculated and abiotic culture medium in the presence or absence of lactate as an organic electron donor over 8 days (Fig. 4A). Under abiotic conditions (sterile electrolyte), the organic electron donor had no influence on the potential. Therefore, we chose to present only curve of controls in medium containing lactate (Fig. 4A). Within the first few hours, the E_{corr} curves of all conditions decreased to more electronegative potentials and increased to more positive values after one day. In *A. fulgidus*-inoculated media with lactate, lowest E_{corr} potentials were observed after one day of stabilization in comparison to other conditions. The abiotic control reached, approximately, −480 mV/SCE from day 3 and remained stable until day 5. It showed abrupt decrease to reach −600mV/SCE. However, it increased at day 6 to gain the initial level of −480 mV/SCE again. These abrupt decrease and increase corresponded to an artifact. A similar but smaller artifact was also observed few hours later in the *A. fulgidus*-inoculated assay without lactate; however, the artifact was not detected in the assay with lactate. In the absence of lactate as an

Table 1
Elements composition of crust deposits on metal surfaces by Energy-Dispersive X-ray spectroscopy analysis. Presentation of mass percent and Atomic percent of elements. *nd*: non detected.

Abiotic control		
Elements	**Mass (%)**	**Atomic (%)**
C	20.7	34.1
O	37.0	45.7
Na	2.9	2.5
Mg	4.8	3.9
Si	0.4	0.3
S	1.9	1.2
Cl	1.6	0.9
Ca	4.6	2.3
Fe	26.1	9.2
Total:	100	100
Tangled material		
Elements	**Mass (%)**	**Atomic (%)**
C	12.5	27.7
O	14.1	23.4
Na	8.0	9.2
Mg	1.2	1.3
Si	2.7	2.6
S	14.7	12.3
Cl	4.5	3.4
Ca	*nd*	*nd*
Fe	42.4	20.2
Total:	100	100
Chimney		
Elements	**Mass (%)**	**Atomic (%)**
C	16.9	32.7
O	24.6	35.7
Na	8.1	8.2
Mg	1.6	1.5
Si	*nd*	*nd*
S	1.0	0.7
Cl	5.0	3.3
Ca	*nd*	*nd*
Fe	42.8	17.8
Total:	100	100

electron donor, the E_{corr} showed a slight increase compared to the abiotic condition before day 1. However, this increase does not last as E_{corr} reached −550 mV/SCE at day 2 and remained stable without any variation. When lactate was added to the *A. fulgidus*-inoculated medium, E_{corr} values were even more negative (−650 mV/SCE) compared to the *A. fulgidus*-inoculated medium lacking lactate (Fig. 4A). These data suggest that the presence of *A. fulgidus* leads to more electronegative potential and hence to electron uptake from the metal as it is corrosive.

3.4.2. *A. fulgidus current-potential response to corrosion*

After day 8 of culture in the corrosion cell, open circuit potential measurements (Fig. 4A) were stopped and followed by potentiodynamic characterization to assess corrosion rate (Fig. 4B). The potentiodynamic curves obtained allowed the extrapolation of Tafel's slopes from which the corrosion current densities were calculated (i_{corr}). Current densities of approximately 80, 105 and 500 μA/cm^2 were obtained for the abiotic control and assays without and with lactate, respectively (Fig. 4B). In the *A. fulgidus*-inoculated condition containing lactate, the corrosion current density was six times greater than that of the abiotic control and five times higher than that of *A. fulgidus* with iron coupon as the only electron donor. Besides, passivation phenomena were observed for the microbial assays that were greater in the medium lacking lactate (Fig. 4B). Thus, the presence of the archaeon increase corrosion rate.

3.5. *A. fulgidus microbial activity*

Lactate and sulfate consumption as well as the formation of Fe^{2+} from Fe^0 oxidation were monitored over a month of incubation at 70 °C with the aim to evaluate Fe^0 oxidation and corrosion processes due to sulfide production. In these experimental settings, we added *A. fulgidus*-inoculated controls without iron coupon, with sulfate and with or without lactate. In assays containing lactate and an iron coupon, the Fe^{2+} concentration increased drastically up to four times than what detected in the abiotic control (Fig. 5A). The higher concentration was reached around day 4 and further increased until the end of the monitoring (Fig. 5A). In *A. fulgidus*-inoculated assays containing iron coupon only, the concentration of Fe^{2+} slowly increased. Only after 4 days of incubation, it was different of that of the abiotic control and then became two times greater than that of the abiotic control (Fig. 5A). Interestingly, under these lithotrophic conditions, no sulfate consumption was detected (Fig. 5C) and small amounts of acetate were produced leading to the accumulation of about 0.9 mM acetate at the end of the experiment (Fig. 5D). Although, the culture medium contained 0.1 g.L^{-1} yeast extract, *A. fulgidus* was not able to grow and no acetate was produced in absence of an iron coupon (data not shown). All these results

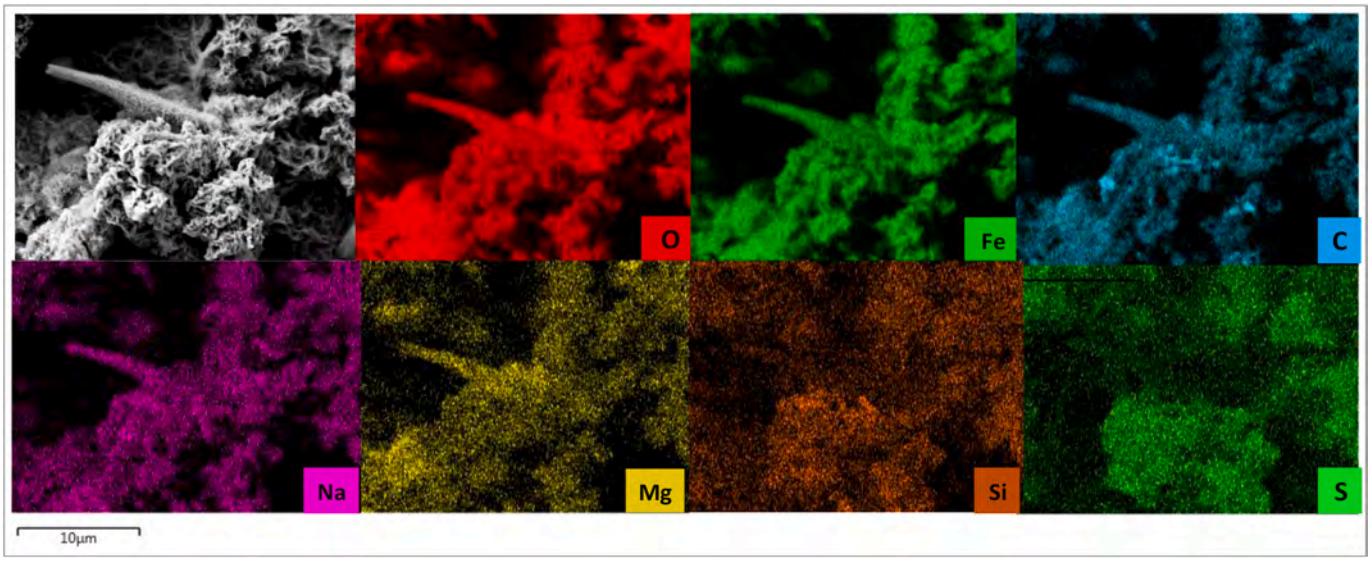

Fig. 2. Scanning electron micrograph (SEM) and X-ray microanalysis (EDX maps) of a chimney observed after the exposure of an iron specimen to a culture of *A. fulgidus* for 3 weeks in the absence of lactate as an electron donor. (EHT = 5 kV, 4.00KX).

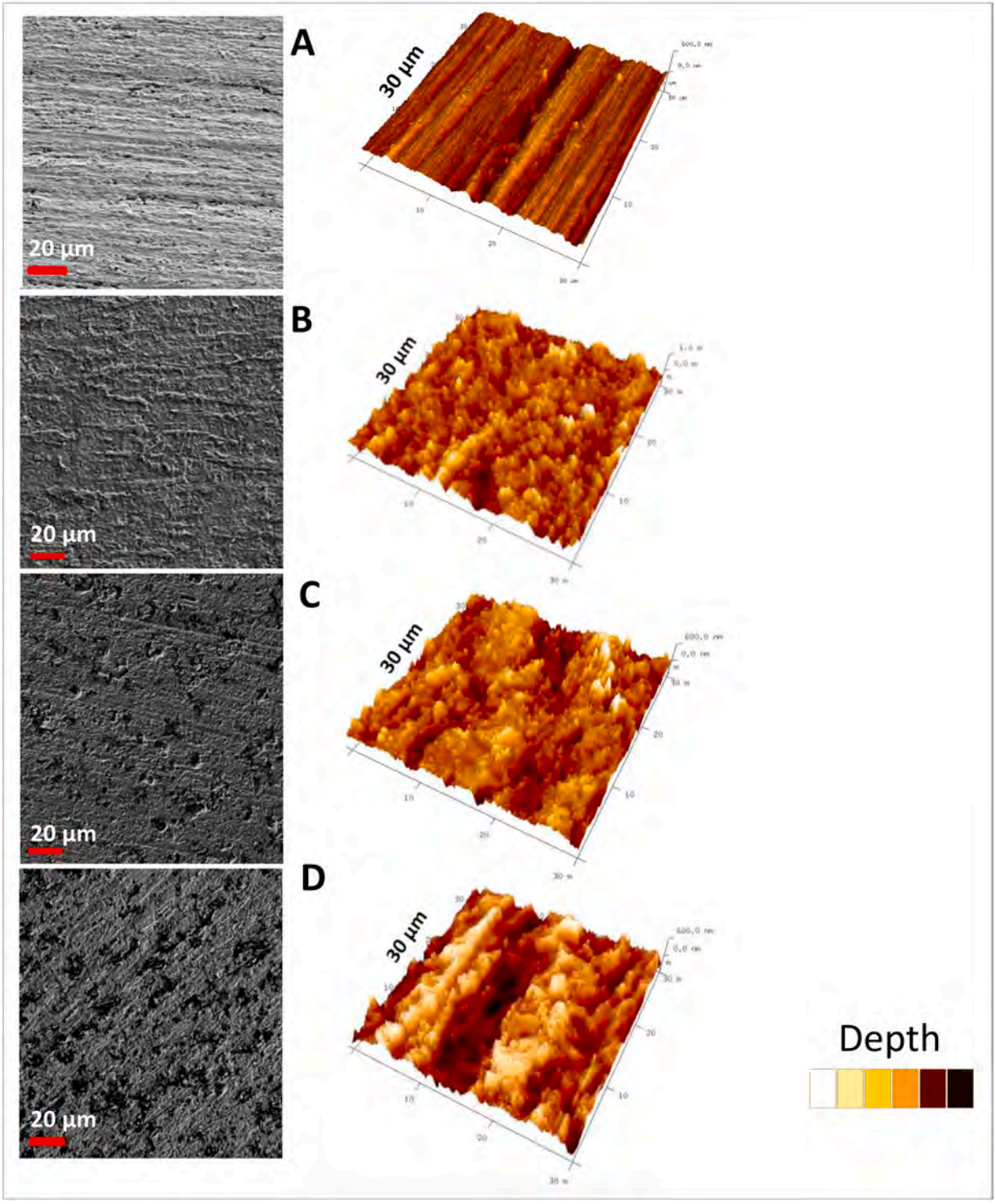

Fig. 3. Corrosion pits on iron steel SEM micrographs (left) and their corresponding 3D AFM images (right) obtained after 3 weeks of incubation. Corrosion crusts were removed before observation. (A) Unincubated metal reference; (B) abiotic control; (C) *A. fulgidus* without lactate and (D) *A. fulgidus* with lactate.

suggest that acetate production should result from lithotrophic growth on iron with CO_2 to be used as terminal electron acceptor. Under organotrophic conditions, kinetics of the lactate oxidized and the sulfate reduced were a little faster in *A. fulgidus*-inoculated controls without iron coupon than in assays with iron. Indeed, in the absence of iron, all the lactate was consumed after 5 days of incubation while small amounts remained even after 10 days in its presence (Fig. 5B). These results suggest that lactate oxidation is delayed in presence of iron. However, in both cases, the redox ratio was around 1.2 sulfate reduced per lactate oxidized (Fig. 5B and C). Interestingly, when *A. fulgidus* was grown with lactate and an iron coupon, acetate production occurred concomitantly to the consumption of lactate (Fig. 5D) from the 2nd day until the 6th day. Following this fast acetate production, the production continues with the kinetic tendency of the assay under lithotrophic growth condition. The acetate concentration reached a maximum of 1.45 mM at day 13 and then decreased slightly (1 mM remaining at day 32). Thus, acetate was first accumulated and slowly consumed afterwards when the medium became lactate deficient (after day 13). The increase of acetate

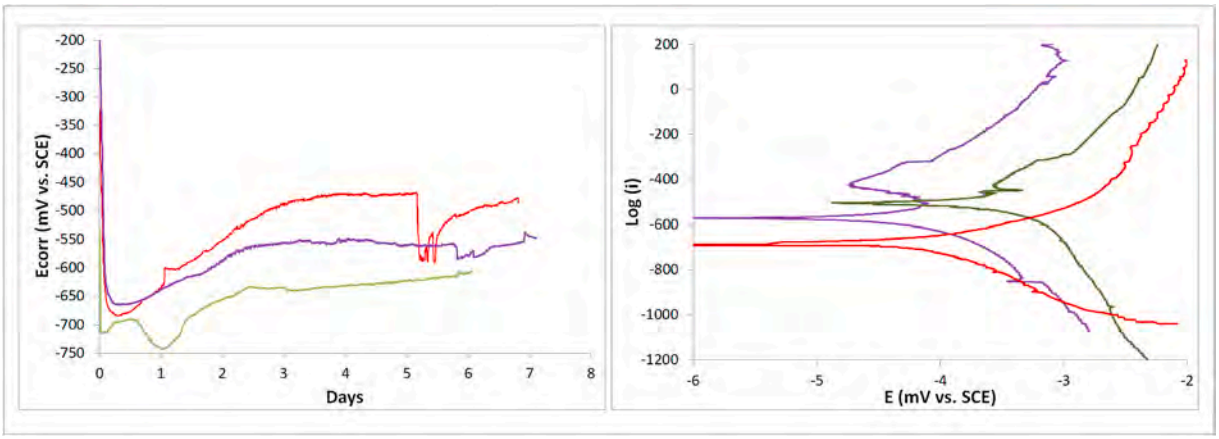

Fig. 4. Monitoring of the corrosion by electrochemical process. A) Kinetics of the open circuit potential vs. the saturated calomel electrode (SCE). B) Potentiodynamic curves performed vs. SCE (scan rate 0.166 mV s^{-1}). ■ Abiotic control; ■ *A. fulgidus* without lactate; and ■ *A. fulgidus* with lactate.

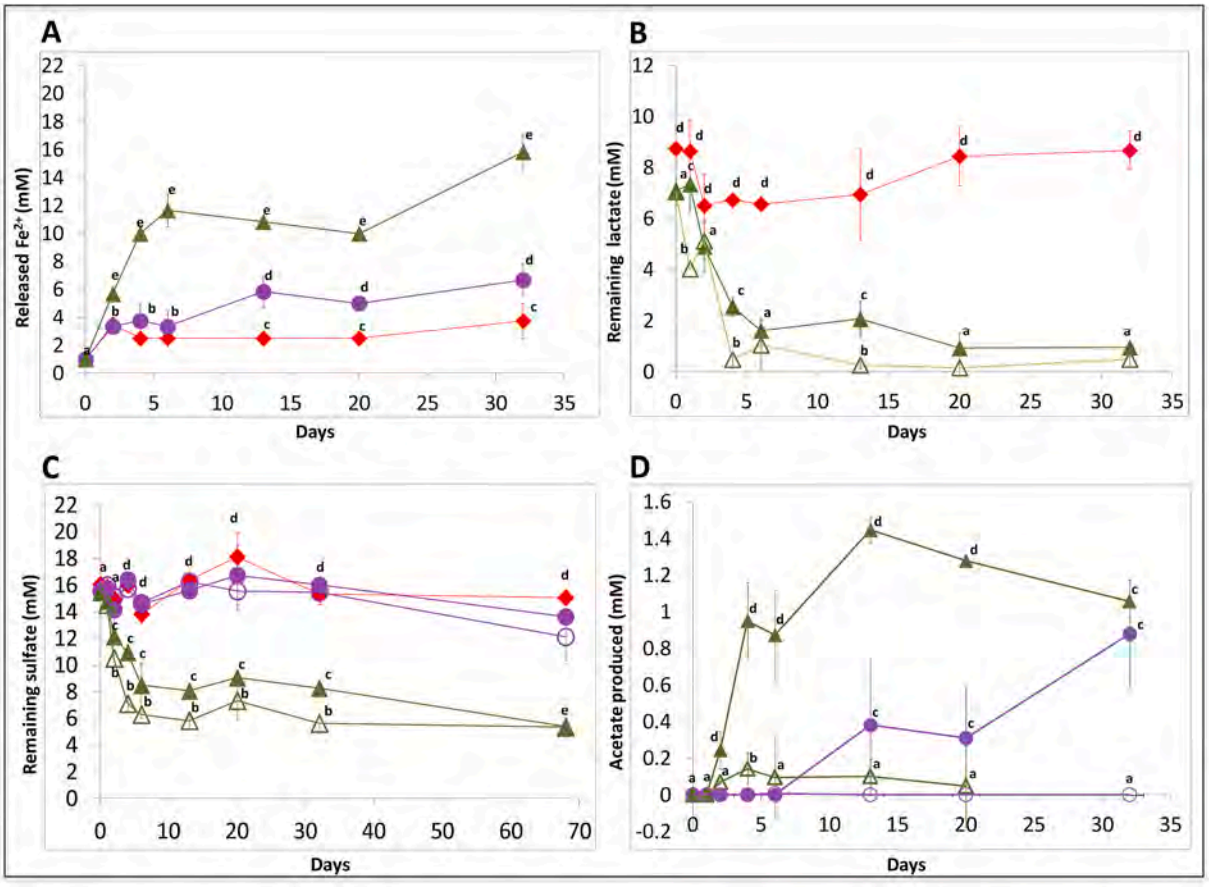

Fig. 5. Physiology of *A. fulgidus* in the presence and absence of an iron coupon. Fe^{2+} released (A), remaining lactate (B) and sulfate (C), and acetate produced (D). ◆ Abiotic control with iron steel; ▲ *A. fulgidus* with an iron coupon and lactate; △ *A. fulgidus* with lactate and without an iron coupon; ● *A. fulgidus* with an iron coupon and without lactate; and ○ *A. fulgidus* without an iron coupon and without lactate. Statistical analyses were performed using a multifactor analysis of variance (ANOVA) followed by a Fisher's least significant difference (LSD) procedure to assess significant differences among the conditions. [a, b, c, d, e] Significant differences for the Fe^{2+}, lactate and sulfate ($p < 0.000$) and acetate ($p < 0.0001$) concentrations.

concentration between day 6 and 13, seemed to follow the same tendency of the lithotrophic condition.

4. Discussion

While Lapaglia and Hartzel (Lapaglia and Hartzell, 1997) demonstrated that *A. fulgidus* VC-16 was able to form different biofilm structures after 12–18 h under a high concentration of nickel, here we establish that when grown on iron coupon as a sole mineral energy source. This hyperthermophilic archaeon formed tangled materials (Fig. 1C–D) also corresponding to a microbial biofilm (Motos et al., 2015; Rastelli et al., 2016)This biofilm was much more developed in the presence of lactate as an organic carbon and energy source.

Indeed, after crust removal, the pits observed on iron surface (Fig. 3)

indicate the ability of *A. fulgidus* to corrode iron either in the presence or absence of lactate as an organic electron donor although pits were wider and deeper when lactate was added. These observations are supported by electrochemical analysis (Fig. 4). Actually, in terms of thermodynamic tendency, a more negative E_{corr} indicates that the working electrode is more prone to donate electrons. Throughout the experiment, the most substantial electronegative potentials were observed for the *A. fulgidus*-inoculated assays and more importantly in assays with lactate (Fig. 4). These lower measured potentials of *A. fulgidus*-inoculated media correspond to an accelerated corrosion process (Venzlaff et al., 2013; Wu et al., 2015; Raman et al., 2008; Cheng et al., 2009; Alfaro-Cuevas-Villanueva et al., 2006), confirmed by our measured current densities. It could be related to intense microbial activity (Cheng et al., 2009) and correlated to the SEM and AFM observations (Figs. 1C and 3D). The evolution of the E_{corr} to more cathodic potentials was a consequence of the biofilm formation, the development of associated corrosion products (Fig. 1B–D) and the passivation phenomena also observed on polarization curves (Fig. 4B). In addition to biofilm establishment, cell growth can lead to the production of corrosive metabolites such as sulfides (Cheng et al., 2009). In presence of lactate, passivation phenomena were weakened by the intense microbial activity. The passivation that developed in the absence of lactate could be due to a more stable layer of corrosion products. The anodic corrosion potentials (Fig. 4A) and current densities (Fig. 4B) supported all these results and confirmed an oxidation state of Fe^0. Hence, corrosiveness could be related to indirect processes (e.g., sulfide production) and to direct mechanisms (e.g., metal oxidation).

In the absence of lactate, a thin microbial biofilm with chimneys developed on the iron coupon after 3 weeks of incubation (Fig. 1D). Recently, similar chimneys were also observed for the first time, in the absence of an organic electron donor with the mesophilic sulfate-reducing bacterium, *Desulfopila corrodens* (Enning et al., 2012; Dinh et al., 2004). The *D. corrodens* chimneys structures took 3 months to form at 28 °C and pH ≥ 9. They were considered to be ion conductive precipitates composed of FeS and $FeCO_3$ and were suggested to allow ion flow from the dissolving iron into the bacterial cells (Enning and Garrelfs, 2014; Venzlaff et al., 2013). The chimneys observed in the *A. fulgidus* VC-16 inoculated-assays were thinner than those of *D. corrodens* and formed within only 2–3 weeks at 70 °C. Moreover, those formed by *A. fulgidus* were observed in medium at pH7. Therefore, the chimney formation rate of *A. fulgidus* may be linked to higher temperatures and/or differences in pH. The S and Si elements were specifically coupled to the microbial biofilm (Alfaro-Cuevas-Villanueva et al., 2006) underneath the *A. fulgidus* chimneys. In contrast, S was found in the chimney composites formed by *D. corrodens* (Enning et al., 2012). All together, these results suggest that the chimneys formed by *A. fulgidus* differed slightly from those of *D. corrodens* since there is no FeS in the composition of the *A. fulgidus* VC-16 chimneys (Fig. 2). Chimney structures were not observed in the assays containing lactate (Fig. 1C). Under the latter condition, we can expect that chimneys did not form or the dense microbial biofilm or precipitates covered these chimneys. Nevertheless, it is clear from our experiments that these chemical structures result from microbial activity on iron coupons.

Besides the observation of biofilm and chimney formation, we demonstrate that *A. fulgidus* VC16 can use the iron coupon (Fe^0) as a sole electron donor oxidizing it to Fe^{2+} similarly to other anaerobic microorganisms such as iron-oxidizing microorganisms and few sulfate-reducing bacteria. Thus, our results confirm the previous study of Jia and coworkers (2018) who had established corrosive activity of *A. fulgidus* VC16 under carbon starvation (Jia et al., 2018). Moreover, we showed that growth of *A. fulgidus* (e.g., biofilm formation) in iron-containing assays without lactate was not linked to sulfate reduction (Figs. 1D and 5C). Interestingly, small amounts of acetate accumulated under these conditions (Fig. 5D). Previous studies by Henstra and coworkers (2007) revealed that *A. fulgidus* may perform homoacetogenesis using CO as an energy source either in the presence or absence of sulfate. They also demonstrated that CO_2 may be used as a terminal electron acceptor by this microorganism to produce acetate (Henstra et al., 2007). In this respect, under the above-mentioned culture conditions, we propose that *A. fulgidus* could oxidize iron by using CO_2 as terminal electron acceptor through the Wood-Ljungdahl metabolic pathway with acetate being an end-product of metabolism (homoacetogenesis), thus bypassing the reduction of SO_4^{2-}. The net reaction below (3) would therefore correspond to the combination of the two half-reactions (1) and (2):

$$2\ HCO_3^- + 9\ H^+ + 8\ e^- \leftrightarrow CH_3COO^- + 4\ H_2O \quad (2)$$

$$4\ Fe^0 + 2\ HCO_3^- + 9\ H^+ \leftrightarrow CH_3COO^- + 4\ Fe^{2+} + 4\ H_2O \quad (3)$$

Indeed, from day 13–32, the acetate concentration produced and Fe^{2+} released (Fig. 5A–D) are in accordance with equation (3). In this respect, we could hypothesize that under our culture conditions, *A. fulgidus* could grow lithoautotrophically on iron steel using dissolved CO_2 as a terminal electron acceptor instead of sulfate. Such conclusion is reinforced by the fact that *A. fulgidus* is known to be able to use hydrogen, and consequently electrons delivered from hydrogen oxidation only when thiosulfate, but not sulfate served as terminal electron acceptor (Hocking et al., 2014). The absence of sulfate consumption in such culture conditions is also supported by the absence of FeS in the chimneys. Nevertheless, supplementary studies would be necessary to deepen this hypothesis.

In the presence of lactate, a more complex scenario was observed. The analysis of *A. fulgidus*-inoculated controls (no iron) shows that the ratio sulfate/lactate consumed was stable and was around 1.3 from early days. Thus, considering that a part of the lactate used is incorporated in the biomass as carbon source, the balance sheet is in accordance with a complete oxidation of lactate according to the following stoichiometric equation (Stetter, 1988; Möller-Zinkhan and Thauer, 1990), as already reported for *A. fulgidus* (Stetter, 1988):

$$CH_3\text{–}CHOH\text{–}COO^- + 1.5\ SO_4^{2-} \rightarrow 3\ HCO_3^- + 1.5\ HS^- + 0.5\ H^+ \quad (4)$$

Nonetheless, in the assays containing both lactate and iron, acetate accumulated concomitantly to the oxidation of lactate (Fig. 5 B and D). Herein, we suggest that lactate oxidation was no more complete as in stoichiometric equation (4) because acetate accumulated even poorly. Hence, the ratio of sulfate/lactate (around 1.2) and the acetate produced (Fig. 5D) would approximately correspond to the stoichiometric equation below:

$$CH_3\text{–}CHOH\text{–}COO^- + 1.33\ SO_4^{2-} \rightarrow 0.17\ CH_3COO^- + 1.33\ HS^- + 2.66\ HCO_3^- + 0.5\ H^+ \quad (5)$$

Moreover, acetate produced after the depletion of lactate (from day 6 to day 13) would result from homoacetogenesis with iron, corresponding to the reaction (3). This hypothesis is supported by the stabilization of the remaining sulfate concentration. The total acetate produced could be attributed, therefore, to direct corrosion process. Thus, we can suggest that direct corrosion may occur concomitantly to indirect corrosion in *A. fulgidus*-inoculated assays containing lactate when cells adhere to the metallic surface. *A. fulgidus* might use acetate as carbon and/or energy source, as already reported for *Archaeoglobus veneficus* (Huber et al., 1997) and *Archaeoglobus profundus* (Burggraf et al., 1990), respectively. Yet, these metabolic features have not been reported for *A.fulgidus* so far. Overall, iron presence slightly affects *A. fulgidus* metabolism leading to the incomplete oxidation of lactate.

We propose a schematic mechanism to illustrate electron flow from Fe^0 to *A. fulgidus* cells in the presence and absence of lactate (Fig. 6). In the presence of lactate (Fig. 6A), *A. fulgidus* enables indirect iron corrosion through the secretion of corrosive sulfide that chemically attacks the iron coupon. The archaeon may also oxidize iron directly as the metabolism is modified in the presence of an iron coupon. The latter possibility is not shown. In Fig. 6B, a schematic mechanism illustrates

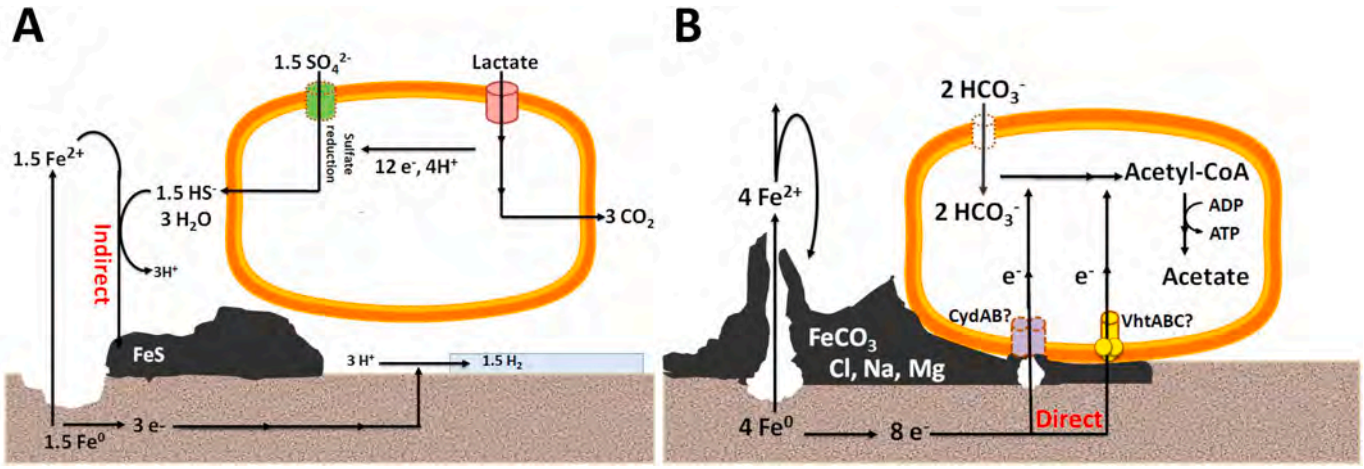

Fig. 6. Schematic proposal of the *A. fulgidus* corrosion mechanisms in the presence of lactate (A) and with iron metal only (B). CydAB: cytochrome *bc* oxidase; VhtABC: periplasmic hydrogenase; ATP: adenosine triphosphate; ADP: adenosine diphosphate.

how *A. fulgidus* VC-16 can act as a direct Fe^0 oxidizer. First, we must take into account the known key roles of hydrogenases and cytochromes in direct electron transfer (Van Ommen Kloeke et al., 1995; Mehanna et al., 2009; Hernandez and Newman, 2001; Deutzmann et al., 2015). *A. fulgidus* has been recognized to possess several cytochromes (Klenk et al., 1997) such as cytochrome-C_3 hydrogenase, which is known to be an excellent electron carrier (Van Ommen Kloeke et al., 1995; Booth G and Tiller, 1960), as well as two hydrogenases, one of which is periplasmic (Hocking et al., 2015). The involvement of hydrogenase in direct electron uptake is not new. Indeed, microorganisms like *Desulfovibrio vulgaris* Hildenborough, for example, have already been shown to uptake electron directly from iron and transfer it to periplasmic hydrogenase (Van Ommen Kloeke et al., 1995). In addition, chimneys formed by *A. fulgidus* may act as ion bridges to enable direct electron uptake from the iron coupon by the archaeal cells.

5. Conclusion

Our study provides evidence that *A. fulgidus* VC-16 possess the ability to corrode iron indirectly by producing sulfide while oxidizing lactate and directly by oxidizing iron steel. Throughout our study, we glimpse the many metabolic possibilities of *A. fulgidus* modulated by the presence of iron and also by the presence or absence of a suitable organic electron donor. Moreover, we provide evidence that *A. fulgidus*, which possibly thrives in hot oil reservoirs (Davidova et al., 2012; Duncan et al., 2009; Cord-Ruwisch et al., 1987), may be a highly corrosive microbial agent possibly damaging oilfield facilities in terms of oil reservoir souring similarly to other sulfate-reducing bacteria. Further work is needed to clearly identify the economic losses in the oil industry that are due to its presence in deep hot petroleum reservoirs (Davidova et al., 2012; Duncan et al., 2009).

Declaration of competing interest

The authors declare that they have no known competing financial interests or personal relationships that could have appeared to influence the work reported in this paper.

Acknowledgements

This work was partially supported by the French CNRS-INSU grant for the BIOHYDEX EC2CO-Microbien project. The laboratories of the MIO, Aix-Marseille University, where most of the experiments were performed, are in compliance with ISO9001-2015.

Appendix A. Supplementary data

Supplementary data to this article can be found online at https://doi.org/10.1016/j.ibiod.2020.105056.

References

Alfaro-Cuevas-Villanueva, R., Cortes-Martinez, R., García-Díaz, J.J., Galvan-Martinez, R., Torres-Sanchez, R., 2006. Microbiologically influenced corrosion of steels by thermophilic and mesophilic bacteria. Mater. Corros. 57 (7), 543–548. https://doi.org/10.1002/maco.200503948.

Balch, W.E., Fox, G.E., Magrum, L.J., Woese, C.R., Wolfe, R.S., 1979. Methanogens: reevaluation of a unique biological group. Microbiol. Rev. 43 (2), 260.

Beech, I.B., Sunner, J., 2004. Biocorrosion: towards understanding interactions between biofilms and metals. Curr. Opin. Biotechnol. 15 (3), 181–186. https://doi.org/10.1016/j.copbio.2004.05.001.

Beeder, J., Nilsen, R.K., Rosnes, J.T., Torsvik, T., Lien, T., 1994. *Archaeoglobus fulgidus* isolated from hot North Sea oil field waters. Appl. Environ. Microbiol. 60 (4), 1227–1231.

Booth G, H., Tiller A, K., 1960. Polarization studies of mild steel in cultures of sulphate-reducing bacteria. J. Chem. Soc. Faraday. Trans. 56 https://doi.org/10.1039/tf9605601689.

Burggraf, S., Jannasch, H.W., Nicolaus, B., Stetter, K.O., 1990. *Archaeoglobus profundus* sp. nov., represents a new species within the sulfate-reducing Archaebacteria. Syst. Appl. Microbiol. 13, 24–28, 80176-1.

Cheng, S., Tian, J., Chen, S., Lei, Y., Chang, X., Liu, T., Yin, Y., 2009. Microbially influenced corrosion of stainless steel by marine bacterium *Vibrio natriegens*: (I) corrosion behavior. Mater. Sci. Eng. C 29 (3), 751–755. https://doi.org/10.1016/j.msec.2008.11.013.

Cord-Ruwisch, R., Widdel, F., 1986. Corroding iron as a hydrogen source for sulphate reduction in growing cultures of sulphate-reducing bacteria. Appl. Microbiol. Biotechnol. 25 (2), 169–174. https://doi.org/10.1007/bf01982842.

Cord-Ruwisch, R., Kleinitz, W., Widdel, F., 1987. Sulfate-reducing bacteria and their activities in oil production. J. Petrol. Technol. 39 (1), 97–106. https://doi.org/10.2118/13554-PA.

Costello, J.A., 1974. Cathodic depolarization by sulfate-reducing bacteria. S. Afr. j. sci. 70 (7), 202–204.

Dang, H., Lovell, C.R., 2016. Microbial surface colonization and biofilm development in marine environments. Microbiol. Mol. Biol. Rev. 80 (1), 91–138. https://doi.org/10.1128/MMBR.00037-15.

Davidova, I.A., Duncan, K.E., Perez-Ibarra, B.M., Suflita, J.M., 2012. Involvement of thermophilic archaea in the biocorrosion of oil pipelines. Environ. Microbiol. 14 (7), 1762–1771. https://doi.org/10.1111/j.1462-2920.2012.02721.x.

Deutzmann, J.S., Sahin, M., Spormann, A.M., 2015. Extracellular enzymes facilitate electron uptake in biocorrosion and bioelectrosynthesis. mBio 6 (2). https://doi.org/10.1128/mBio.00496-15.

Dinh, H.T., Kuever, J., Mussmann, M., Hassel, A.W., Stratmann, M., Widdel, F., 2004. Iron corrosion by novel anaerobic microorganisms. Nature 427 (6977), 829–832. https://doi.org/10.1038/nature02321.

Duncan, K.E., Gieg, L.M., Parisi, V.A., Tanner, R.S., Tringe, S.G., Bristow, J., Suflita, J.M., 2009. Biocorrosive thermophilic microbial communities in Alaskan North slope oil facilities. Environ. Sci. Technol. 43 (20), 7977–7984. https://doi.org/10.1021/es9013932.

Enning, D., Garrelfs, J., 2014. Corrosion of iron by sulfate-reducing bacteria: new views of an old problem. Appl. Environ. Microbiol. 80 (4), 1226–1236. https://doi.org/10.1128/AEM.02848-13.

Enning, D., Venzlaff, H., Garrelfs, J., Dinh, H.T., Meyer, V., Mayrhofer, K., Hassel, A.W., Stratmann, M., Widdel, F., 2012. Marine sulfate-reducing bacteria cause serious corrosion of iron under electroconductive biogenic mineral crust. Environ. Microbiol. 14 (7), 1772–1787. https://doi.org/10.1111/j.1462-2920.2012.02778.x.

Fardeau, M.-L., Goulhen, F., Bruschi, M., Khélifi, N., Cayol, J.L., Ignatiadis, I., Guyot, F., Ollivier, B., 2009. *Archaeoglobus fulgidus* and *Thermotoga elfii*, thermophilic isolates from deep geothermal water of the Paris basin. Geomicrobiol. J. 26 (2), 119–130. https://doi.org/10.1080/01490450802674970.

Hamilton, W.A., 2003. Microbially influenced corrosion as a model system for the study of metal microbe interactions: a unifying electron transfer hypothesis. Biofouling 19 (1), 65–76. https://doi.org/10.1080/0892701021000041078.

Henstra, A., Dijkema, C., Stams A, J.M., 2007. *Archaeoglobus fulgidus* couples CO oxidation to sulfate reduction and acetogenesis with transient formate accumulation. Environ. Microbiol. 9, 1836–1841. https://doi.org/10.1111/j.1462-2920.2007.01306.x.

Hernandez, M.E., Newman, D.K., 2001. Extracellular electron transfer. Cell. Mol. Life Sci. 58 (11), 1562–1571. https://doi.org/10.1007/PL00000796.

Hocking, W., Stokke, R., Roalkvam, I., Steen, I., 2014. Identification of key components in the energy metabolism of the hyperthermophilic sulfate-reducing archaeon *Archaeoglobus fulgidus* by transcriptome analyses. Front. Microbiol. 5, 95. https://doi.org/10.3389/fmicb.2014.00095.

Hocking, W., Roalkvam, I., Magnussen, C., Stokke, R., Steen, I., 2015. Assessment of the carbon monoxide metabolism of the hyperthermophilic sulfate-reducing archaeon *Archaeoglobus fulgidus* VC-16 by comparative transcriptome analyses. Archaea 2015, 1–12. https://doi.org/10.1155/2015/235384.

Huber, H., Jannasch, H., Rachel, R., Fuchs, T., Stetter, K.O., 1997. *Archaeoglobus veneficus* sp. nov., a novel facultative chemolithoautotrophic hyperthermophilic sulfite reducer, isolated from Abyssal black smokers. Syst. Appl. Microbiol. (20), 374–380, 80005-7.

Hubert, C., Nemati, M., Jenneman, G., Voordouw, G., 2005. Corrosion risk associated with microbial souring control using nitrate or nitrite. Appl. Microbiol. Biotechnol. 68 (2), 272–282. https://doi.org/10.1007/s00253-005-1897-2.

Islam, S., Karr, E.A., 2013. Examination of metal corrosion by *Desulfomicrobium thermophilum, Archaeoglobus fulgidus*, and *Methanothermobacter thermautotrophicus*. BIOS 84 (2), 59–64. https://doi.org/10.1893/0005-3155-84.2.59.

Jia, R., Yang, D., Xu, D., Gu, T., 2018. Carbon steel biocorrosion at 80 °C by a thermophilic sulfate reducing archaeon biofilm provides evidence for its utilization of elemental iron as electron donor through extracellular electron transfer ». Corrosion Sci. 145, 47–54. https://doi.org/10.1016/j.corsci.2018.09.015.

Kaesche, H., 2012. Corrosion of Metals: Physicochemical Principles and Current Problems. Springer Science Business Media. https://doi.org/10.1007/978-3-642-96038-3.

Kato, S., Yumoto, I., Kamagata, Y., 2015. Isolation of acetogenic bacteria that induce biocorrosion by utilizing metallic iron as the sole electron donor. Appl. Environ. Microbiol. 81 (1), 67–73. https://doi.org/10.1128/AEM.02767-14.

Khelifi, N., Grossi, V., Hamdi, M., Dolla, A., Tholozan, J.-L., Ollivier, B., Hirschler-Réa, A., 2010. Anaerobic oxidation of fatty acids and alkenes by the hyperthermophilic sulfate-reducing archaeon *Archaeoglobus fulgidus*. Appl. Environ. Microbiol. 76 (9), 3057–3060. https://doi.org/10.1128/AEM.02810-09.

Khelifi, N., Ali, O.A., Roche, P., Grossi, V., Brochier-Armanet, C., Valette, O., Ollivier, B., Dolla, A., Hirschler-Réa, A., 2014. Anaerobic oxidation of long-chain n-alkanes by the hyperthermophilic sulfate-reducing archaeon, *Archaeoglobus fulgidus*. ISME J. 8 (11), 2153–2166. https://doi.org/10.1038/ismej.2014.58.

Klenk, H.-P., Clayton, R.A., Tomb, J.-F., White, O., Nelson, K.E., Ketchum, K.A., Dodson, R.J., Gwinn, M., Hickey, E.K., Peterson, J.D., Richardson, D.L., Kerlavage, A.R., Graham, D.E., Kyrpides, N.C., Fleischmann, R.D., Quackenbush, J., Lee, N.H., Sutton, G.G., Gill, S., Kirkness, E.F., Dougherty, B.A., McKenney, K., Adams, M.D., Loftus, B., Peterson, S., Reich, C.I., McNeil, L.K., Badger, J.H., Glodek, A., Zhou, L., Overbeek, R., Gocayne, J.D., Weidman, J.F., McDonald, L., Utterback, T., Cotton, M.D., Spriggs, T., Artiach, P., Kaine, B.P., Sykes, S.M., Sadow, P.W., D'Andrea, K.P., Bowman, C., Fujii, C., Garland, S.A., Mason, T.M., Olsen, G.J., Fraser, C.M., Smith, H.O., Woese, C.R., Venter, J.C., 1997. The complete genome sequence of the hyperthermophilic, sulphate-reducing archaeon *Archaeoglobus fulgidus*. Nature 390 (6658), 364–370. https://doi.org/10.1038/37052.

L'Haridon, S., Reysenbacht, A.L., Glénat, P., Prieur, D., Jeanthon, C., 1995. Hot subterranean biosphere in a continental oil reservoir. Nature 377 (6546), 223–224. https://doi.org/10.1038/377223a0.

Lapaglia, C., Hartzell, P.L., 1997. Stress-induced production of biofilm in the hyperthermophile *Archaeoglobus fulgidus*. Appl. Environ. Microbiol. 63 (8), 3158–3163.

Liang, R., Grizzle, R.S., Duncan, K.E., McInerney, M.J., Suflita, J.M., 2014. Roles of thermophilic thiosulfate-reducing bacteria and methanogenic archaea in the biocorrosion of oil pipelines. Front. Microbiol. 5 https://doi.org/10.3389/fmicb.2014.00089.

Liang, R., Aktas, D.F., Aydin, E., Bonifay, V., Sunner, J., Suflita, J.M., 2016. Anaerobic biodegradation of alternative fuels and associated biocorrosion of carbon steel in marine environments. Environ. Sci. Technol. 50 (9), 4844–4853. https://doi.org/10.1021/acs.est.5b06388.

Liengen, T., Basseguy, R., Feron, D., Beech, I., Birrien, V., 2014. Understanding Biocorrosion. *Fundamentals and Applications*. Elsevier, p. 447. https://doi.org/10.1016/C2013-0-16468-9.

Lovley, D.R., Phillips, E.J.P., 1986. Organic matter mineralization with reduction of ferric iron in anaerobic sediments. Appl. Environ. Microbiol. 51 (4), 683–689.

Magot, M., Ravot, G., Campaignolle, X., Ollivier, B., Patel, B.K.C., Fardeau, M.L., Thomas, P., Crolet, J.L., Garcia, J.L., 1997. *Dethiosulfovibrio peptidovorans* gen. Nov., sp. nov., a new anaerobic, slightly halophilic, thiosulfate-reducing bacterium from corroding offshore oil wells. Int. J. Syst. Evol. Microbiol. 47 (3), 818–824. https://doi.org/10.1099/00207713-47-3-818.

Mand, J., Park, H.S., Jack, T.R., Voordouw, G., 2014. The role of acetogens in microbially influenced corrosion of steel. Front. Microbiol. 5, 268. https://doi.org/10.3389/fmicb.2014.00268.

Mand, J., Park, H.S., Okoro, C., Lomans, B.P., Smith, S., Chiejina, L., Voordouw, G., 2015. Microbial methane production associated with carbon steel corrosion in a nigerian oil field. Front. Microbiol. 6, 1538. https://doi.org/10.3389/fmicb.2015.01538.

Mehanna, M., Basseguy, R., Delia, M.-L., Bergel, A., 2009. Role of direct microbial electron transfer in corrosion of steels. Electrochem. Commun. 11 (3), 568–571. https://doi.org/10.1016/j.elecom.2008.12.019.

Möller-Zinkhan, D., Thauer, R.K., 1990. Anaerobic lactate oxidation to 3 CO2 by *Archaeoglobus fulgidus* via the carbon monoxide dehydrogenase pathway: demonstration of the acetyl-CoA carbon-carbon cleavage reaction in cell extracts. Arch. Microbiol. 153 (3), 215–218. https://doi.org/10.1007/BF00249070.

Motos, P.R., ter Heijne, A., van der Weijden, R., Saakes, M., Buisman, C.J.N., Sleutels, T. H.J.A., 2015. High rate copper and energy recovery in microbial fuel cells. Front. Microbiol. 6 https://doi.org/10.3389/fmicb.2015.00527.

Ollivier, B., Magot, M., 2005. Petroleum Microbiology. ASM Press, p. 392. https://doi.org/10.1128/9781555817589.

Perez, N., 2004. Electrochemistry and Corrosion Science, vol. 412. Springer. https://doi.org/10.1007/978-3-319-24847-9.

Raman, V., Tamilselvi, S., Rajendran, N., 2008. Evaluation of effective biocides for SRB to control microbiologically influenced corrosion. Mater. Corros. 59 (4), 329–334. https://doi.org/10.1002/maco.200804103.

Rastelli, S.E., Rosales, B.M., Viera, M.R., 2016. Bacterial biofilms formed in arsenic-containing water: bacterial community characterization. J. Water. Supply. Res. T. 65 (1), 1–11. https://doi.org/10.2166/aqua.2015.137.

Sherar, B.W.A., Keech, P.G., Shoesmith, D.W., 2013. The effect of sulfide on the aerobic corrosion of carbon steel in near-neutral pH saline solutions. Corrosion Sci. 66 (Suppl. C), 256–262. https://doi.org/10.1016/j.corsci.2012.09.027.

Stetter, K.O., 1988. *Archaeoglobus fulgidus* gen. nov., sp. nov.: a new taxon of extremely thermophilic archaebacteria. Syst. Appl. Microbiol. 10 (2), 172–173. https://doi.org/10.1016/s0723-2020(88)80032-8.

Stetter, K.O., Huber, R., Blöchl, E., Kurr, M., Eden, R.D., Fielder, M., Cash, H., Vance, I., 1993. Hyperthermophilic archaea are thriving in deep North Sea and Alaskan oil reservoirs. Nature 365 (6448), 743–745. https://doi.org/10.1038/365743a0.

Van Ommen Kloeke, F., Bryant, R.D., Laishley, E.J., 1995. Localization of cytochromes in the outer membrane of *Desulfovibrio vulgaris* (Hildenborough) and their role in anaerobic biocorrosion. Anaerobe 1 (6), 351–358. https://doi.org/10.1006/anae.1995.1038.

Venzlaff, H., Enning, D., Srinivasan, J., Mayrhofer, K.J.J., Hassel, A.W., Widdel, F., Stratmann, M., 2013. Accelerated cathodic reaction in microbial corrosion of iron due to direct electron uptake by sulfate-reducing bacteria. Corrosion Sci. 66, 88–96. https://doi.org/10.1016/j.corsci.2012.09.006.

Videla, H.A., Herrera, L.K., . Microbiologically influenced corrosion: looking to the future. Int. Microbiol. 8 (3), 169–180.

Vigneron, A., Alsop, E.B., Chambers, B., Lomans, B.P., Head, I.M., Tsesmetzis, N., 2016. Complementary microorganisms in highly corrosive biofilms from an offshore oil production facility. Appl. Environ. Microbiol. 82 (8), 2545–2554. https://doi.org/10.1128/AEM.03842-15.

Von Wolzogen Kuehr C, A.H., van der Vlugt L, S., 1964. The Graphitization of cast iron as an electrobiochemical process in anaerobic soils. Water 18, 53.

Vornolt, J., Kunow, J., Stetter, K.O., Thauer, R.K., 1995. Enzymes and coenzymes of the carbon monoxide dehydrogenase pathway for autotrophic CO_2 fixation in *Archaeoglobus lithotrophicus* and the lack of carbon monoxide dehydrogenase in the heterotrophic *A. profundus*. Arch. Microbiol. 163 (2), 112–118. https://doi.org/10.1007/s002030050179.

Wolin, E.A., Wolin, M.J., Wolfe, R.S., 1963. Formation of methane by bacterial extracts. J. Biol. Chem. 238 (8), 2882–2886.

Wu, T.-Q., Yan, M.-C., Zeng, D.-C., Xu, J., Yu, C.-K., Sun, C., Ke, W., 2015. Microbiologically induced corrosion of X80 pipeline steel in a near-neutral pH soil solution. Acta Metal. Sin. Eng. Let. 28 (1), 93–102. https://doi.org/10.1007/s40195-014-0173-9.

Zellner, G., Stackebrandt, E., Kneifel, H., Messner, P., Sleytr, U.B., de Macario, E.C., Zabel, H.-P., Stetter, K.O., Winter, J., 1989. Isolation and characterization of a thermophilic, sulfate-reducing archaebacterium, *Archaeoglobus fulgidus* strain. Z. *Syst. Appl. Microbiol.* 11 (2), 151–160. https://doi.org/10.1016/S0723-2020(89)80055-4.

Zhang, P., Xu, D., Li, Y., Yang, K., Gu, T., 2015. Electron mediators accelerate the microbiologically influenced corrosion of 304 stainless steel by the Desulfovibrio vulgaris biofilm. Bioelectrochemistry 101, 14–21. https://doi.org/10.1016/j.bioelechem.2014.06.010.